






Effect of pH on the self-assembly of three Cd(II) coordination compounds containing 5-(4-pyridyl)tetrazole: syntheses, structures, and properties

Gao-Xiang Meng, Ya-Min Feng, Yin Wang, Yong-Li Gao, Wen-Wu Wan & Xin-Tang Huang

To cite this article: Gao-Xiang Meng, Ya-Min Feng, Yin Wang, Yong-Li Gao, Wen-Wu Wan & Xin-Tang Huang (2015) Effect of pH on the self-assembly of three Cd(II) coordination compounds containing 5-(4-pyridyl)tetrazole: syntheses, structures, and properties, Journal of Coordination Chemistry, 68:10, 1705-1718, DOI: [10.1080/00958972.2015.1024668](https://doi.org/10.1080/00958972.2015.1024668)

To link to this article: <http://dx.doi.org/10.1080/00958972.2015.1024668>

 View supplementary material 

 Accepted author version posted online: 02 Mar 2015.
Published online: 25 Mar 2015.

 Submit your article to this journal 

 Article views: 55

 View related articles 

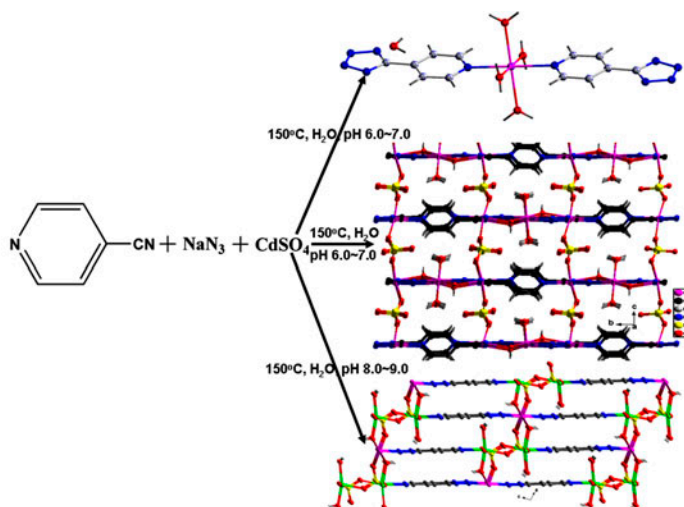
 View Crossmark data 

Effect of pH on the self-assembly of three Cd(II) coordination compounds containing 5-(4-pyridyl)tetrazole: syntheses, structures, and properties

GAO-XIANG MENG, YA-MIN FENG, YIN WANG, YONG-LI GAO,
WEN-WU WAN and XIN-TANG HUANG*

Institute of Nanoscience and Nanotechnology, Department of Physics, Central China Normal University, Wuhan, PR China

(Received 15 October 2014; accepted 9 February 2015)



Three cadmium(II) coordination compounds were synthesized via controlling the pH in the *in situ* [2 + 3] cycloaddition reaction of CdSO₄, 4-cyanopyridine, and sodium azide under hydrothermal treatment. Mononuclear **3** was obtained at weak acid solution pH 6.0–7.0, but 3-D coordination polymers **1** and **2** were preferred in weak alkaline conditions from pH 7.0 to 9.0.

Hydrothermal reactions of CdSO₄, 4-cyanopyridine, and sodium azide yield three metal coordination compounds via controlling the pH, [Cd₂(4-ptz)(SO₄)(OH)(H₂O)₂](H₂O) (**1**) [Cd₂(4-ptz)(SO₄)(OH)(H₂O)]_n (**2**), and known [Cd₂(4-ptz)₂(H₂O)₄](H₂O)₂ (**3**) (4-ptz = 5-(4-pyridyl)tetrazole). The *in situ* [2 + 3] cycloaddition reaction of nitrile and azide in the presence of Cd(II) produces the multidentate 4-ptz in these compounds. X-ray diffraction results indicate that metal centers in **1** are linked by 4-ptz[−], SO₄^{2−}, and OH[−] in their respective μ₅-, μ₂-, μ₃-bridging modes, forming a 3-D coordination polymer. For **2**, although the same raw materials are used, the component anions are linked to Cd

*Corresponding author. Emails: xthuang@phy.ccnu.edu.cn, xintang_huang@126.com

(II) centers in completely different ways, i.e. for 4-ptz⁻ in μ_3^- , SO₄²⁻ in μ_5^- , and OH⁻ in μ_3 -bridging modes, forming another 3-D coordination network. Thermal stabilities and photoluminescent properties of **1** and **2** have also been investigated.

Keywords: Cadmium(II); Coordination polymer; *In situ* synthesis; pH dependent; Fluorescence

1. Introduction

Metal organic supramolecular complexes based on crystal engineering are of current interest due to their potential applications in materials chemistry, biochemistry, environmental science, etc. [1–4]. However, the controllable synthesis of a designed functional metal coordination compound is still a challenge because of factors such as ligand chosen for reaction, the preferred coordination geometry adopted by a metal center, pH, reaction temperature, counter anion, and solvent selected for crystallization affect the final self-assembly structure [5–11]. A good example of this can be provided by a one-pot *in situ* reaction of nitrile/azide/metal and direct reaction between metal and tetrazole conducted by Xiong and coworkers, giving different assembly of metal organic complexes only because of the difference of these initial materials [12]. pH in a reaction system, as one of the external stimuli, is also important in assembly of supramolecular architectures [13–17], affecting a ligand coordination and charge, the metal-to-ligand ratio, and the final structures [8]. For instance, via adjusting the pH in a hydrothermal reaction, Zou *et al.* have prepared mononuclear 5-(4-pyridyl)tetrazole-based cadmium(II) compound [Cd(ptz)₂(H₂O)₄](H₂O)₂ and 1-D polymer [Cd(Hptz)(SO₄)(H₂O)₂]_n under high and low pH media, respectively [18]. Ligands like pyridine–tetrazole, as an important and effective spacer of functional coordination compounds, have been ideal building blocks for multidimensional extended inorganic–organic hybrid materials [3, 5, 6, 9, 19]. They can provide five nitrogen donors coordinating to metal centers and can exhibit two different delocalized aromatic systems from rotation of the C–C single bond between pyridyl and tetrazolyl groups, which may further affect the final polymeric structure via $\pi\cdots\pi$ and/or C–H $\cdots\pi$ interactions.

To further explore the effect of pH on the final assembled supramolecular architecture in this hydrothermal synthesis, we have chosen the initial materials 4-cyanopyridine, sodium azide, and CdSO₄ in the beginning to understand this [2 + 3] *in situ* cycloaddition tetrazole reaction [20, 21]. This one-pot reaction is easily controlled by the pH demonstrated by the final products, {[Cd₂(4-ptz)(SO₄)(OH)(H₂O)₂](H₂O)}_n (**1**), {[Cd₂(4-ptz)(SO₄)(OH)(H₂O)]}_n (**2**), and [Cd(4-ptz)₂(H₂O)₄](H₂O)₂ (**3**). Herein, the synthesis, general characterization, crystal structures, and how their structures are affected by pH are reported in this article.

2. Experimental

2.1. Materials and instrumentations

All chemicals were commercially available reagents of analytical grade and used without purification. Elemental analyses for C, H, and N were performed with a Perkin-Elmer 240C elemental analyzer. IR spectra were obtained on an AVTAR-360 spectrum using KBr disks from 4000 to 400 cm⁻¹. Thermogravimetric analyses (TGA) were studied by a STA 409 PC Luxx in a N₂ atmosphere between room temperature and 1000 °C (heating rate 10 °C min⁻¹). Photoluminescence analyses were performed on an RF-5300PC fluorescence

spectrometer. X-ray powder diffraction measurements were performed on a Bruker D8 Advance diffractometer operated at 40 kV and 40 mA using Cu-K α radiation ($\lambda = 1.54056$ Å). Single-crystal X-ray diffraction was carried out by a Smart Apex CCD diffractometer.

2.2. Synthesis of $\{[Cd_2(4-ptz)(SO_4)(OH)(H_2O)_2](H_2O)\}_n$ (**1**)

In order to obtain a high yield of the final product, the molar ratio of 3-cyanopyridine, NaN₃, and CdSO₄ in the reaction was changed from 1 : 1 : 1 to 1 : 1 : 10 at the beginning of the experiment. Although it was found that in all cases **1** can be obtained, the final yield in *ca.* 1 : 1 : 5 is higher than the other ratios from 1 : 1 : 1 to 1 : 1 : 4. When the stoichiometry ratio exceeds from 1 : 1 : 5 to 1 : 1 : 10, some CdSO₄ salt can be also simultaneously crystallized, which makes the separation of **1** difficult. The 1 : 1 : 5 stoichiometric ratio of 3-cyanopyridine (0.026 g, 0.25 mM), NaN₃ (0.017 g, 0.25 mM), and CdSO₄ (0.26 g, 1.25 mM) were preferred in 18.0 ml distilled water. The mixture was stirred for 20 min at ambient temperature with the pH being adjusted to 7.0–8.0 using 0.01 ML⁻¹ sodium hydroxide water solution and then heated in a 23 ml Teflon-lined reaction vessel at 423 K for 3 d. After slow cooling to room temperature at a rate of 5 K h⁻¹, the product was washed three times with distilled water and collected manually, and air-dried to give colorless block crystals of **1** (0.086 g, yield 64% based on NaN₃). Elem. Anal. Calcd (%): C, 14.39; H, 2.06; N, 13.02; S, 5.96. Found (%): C, 14.41; H, 1.90; N, 13.04; S, 5.97. IR (KBr pellet, cm⁻¹): 3356w, 3256w, 3145s, 3096m, 1948m, 1610m, 1588s, 1440s, 1418m, 1320s, 1208w, 1170m, 1125m, 1050m, 1007m, 958m, 920m, 810m, 748m, 725m, and 680s.

2.3. Synthesis of $\{[Cd_2(4-ptz)(SO_4)(OH)(H_2O)]\}_n$ (**2**)

Compound **2** was synthesized in a similar procedure to **1** except for the pH being adjusted to 8.0–9.0 using 0.01 ML⁻¹ sodium hydroxide water solution. The product gives a yield of *ca.* 41% based on sodium azide (0.051 g). Elem. Anal. Calcd (%): C, 14.35; H, 1.31; N, 13.95; S, 6.39. Found (%): C, 14.36; H, 1.29; N, 13.97; S, 6.41. IR (KBr pellet, cm⁻¹): 3260w, 3150s, 3076m, 1916m, 1629m, 1597m, 1573s, 1473s, 1423m, 1320s, 1203w, 1174m, 1120m, 1047m, 1012m, 910m, 800m, 735m, and 667m.

2.4. Synthesis of $[Cd(4-ptz)_2(H_2O)_4](H_2O)_2$ (**3**)

Compound **3** was synthesized in a similar procedure to **1** except for the pH being adjusted to 6.0–7.0 using 0.01 ML⁻¹ H₂SO₄ water solution. Elem. Anal. Calcd (%): C, 28.11; H, 3.93; N, 27.32. Found (%): C, 28.13; H, 3.85; N, 27.40. IR (KBr, cm⁻¹): 3197w, 3048w, 1620s, 1520s, 1445m, 1383s, 1221w, 1150w, 1040w, 1020w, 860m, 748m, 713w, and 530m.

2.5. X-ray crystallography

All the data-sets for **1–3** were collected on a Smart Apex CCD diffractometer with Mo K α radiation ($\lambda = 0.71073$ Å) by using a ω -2 θ scan mode at ambient temperature. Data reductions were performed using SAINT-Plus [22]. Empirical absorption corrections were applied using the multi-scan program. The structures were solved by direct (or Patterson) methods and refined by full-matrix least-squares on F^2 with anisotropic thermal parameters for all non-hydrogen atoms with the SHELX-97 program [22, 23]. All of the non-hydrogen atoms were refined with anisotropic thermal motion parameters and the contribution of the

Table 1. Crystallographic parameters for **1–3**.

Complexes	1	2	3
Empirical formula	Cd ₂ C ₆ H ₇ O ₆ N ₅ S	Cd ₂ C ₆ H ₁₁ O ₈ N ₅ S	CdC ₁₂ H ₂₀ O ₆ N ₁₀
Formula weight	502.03	538.06	512.78
Temperature (K)	298(2)	298(2)	298(2)
Wavelength (Å)	0.71073	0.71073	0.71073
Crystal system	Monoclinic	Monoclinic	Triclinic
Space group	<i>P</i> 2 ₁ / <i>c</i>	<i>P</i> 2 ₁ / <i>m</i>	<i>P</i> -1
Unit cell dimensions	<i>a</i> = 7.6552(6) Å <i>b</i> = 6.9502(5) Å <i>c</i> = 11.5403(8) Å β = 100.0150(10)°	<i>a</i> = 7.1955(9) Å <i>b</i> = 14.0076(17) Å <i>c</i> = 13.5256(16) Å β = 91.219(2)°	<i>a</i> = 7.3188(10) Å <i>b</i> = 7.8955(11) Å <i>c</i> = 8.8511(12) Å α = 90.414(3)° β = 90.442(3)° γ = 99.698(3)°
Volume (Å ³)	604.65(8)	1363.0(3)	504.12(12)
<i>Z</i>	2	4	1
Density (Calcd Mg m ⁻³)	2.757	2.622	1.689
Absorption coefficient (mm ⁻¹)	3.724	3.324	1.135
<i>F</i> (0 0 0)	476	1032	258
θ range for data collection (°)	2.70–28.29	2.83–26.00	2.30–26.00
Index ranges	-10 ≤ <i>h</i> ≤ 10, 9 ≤ <i>k</i> ≤ 9, -15 ≤ <i>l</i> ≤ 15	-8 ≤ <i>h</i> ≤ 8, -17 ≤ <i>k</i> ≤ 17, -12 ≤ <i>l</i> ≤ 16	-9 ≤ <i>h</i> ≤ 9, -9 ≤ <i>k</i> ≤ 7, -10 ≤ <i>l</i> ≤ 10
Reflections collected	7267	7546	3282
Independent reflections	1606 (<i>R</i> _{int} = 0.0261)	2671 (<i>R</i> _{int} = 0.0750)	1953 (<i>R</i> _{int} = 0.0511)
Data/restraints/parameters	1606/0/112	2671/10/224	1953/9/151
Goodness of fit on <i>F</i> ²	1.192	1.100	0.913
Final <i>R</i> indices [<i>I</i> > 2σ(<i>I</i>)]	<i>R</i> ₁ = 0.0153, <i>R</i> ₂ = 0.0384	<i>R</i> ₁ = 0.0342, <i>R</i> ₂ = 0.0751	<i>R</i> ₁ = 0.0482, <i>R</i> ₂ = 0.0684
<i>R</i> indices (all data)	<i>R</i> ₁ = 0.0154, <i>R</i> ₂ = 0.0385	<i>R</i> ₁ = 0.0382, <i>wR</i> ₂ = 0.0782	<i>R</i> ₁ = 0.0549, <i>R</i> ₂ = 0.0714
Largest diff. peak and hole (e Å ⁻³)	0.473 and -0.640	0.739 and -1.568	0.639 and -0.547

$$R_1 = \Sigma(|F_o| - |F_c|) / \Sigma|F_o|; wR_2 = \{\Sigma[w(F_o^2 - F_c^2)]^2 / \Sigma[w(F_o^2)]\}^{1/2}.$$

carbon-attached hydrogen was included in calculated positions. Water hydrogens were located from the difference maps with O–H and H...H distances constrained by using command “DFIX” in the refinements. The crystallographic parameters are listed in table 1 and some selected bond lengths and angles are listed in table 2. The structural analysis of **1–3** was assisted by the program “PLATON” [24]. Because of **3** being reported earlier [18, 25], its crystal structure will not be mentioned here unless otherwise stated.

3. Results and discussion

3.1. Synthesis of **1–3**

Colorless chunk crystals of **1** and rod-like crystals of **2** (figure S1, see online supplemental material at <http://dx.doi.org/10.1080/00958972.2015.1024668>) are both hydrothermally synthesized by reactions of CdSO₄ with 4-cyanopyridine and sodium azide in molar ratios of 5 : 1 : 1 at 150 °C for 3 days. However, in order to investigate the influence of the acid–base condition conducted in the reaction medium on the final product, the pH value of the pre-reacted solution of **1** is carefully adjusted to weakly alkaline 7.0–8.0 and more strongly alkaline 8.0–9.0 in **2** using water solution of sodium hydroxide (0.01 M) (scheme 1). As a result, the pH has a significant role in shaping these component ions into two different 3-D

Table 2. Some selected bond lengths (Å) and angles (°) for **1–3**.

Complex 1			
Cd1–N4	2.328(3)	Cd2–N3	2.317(3)
Cd1–O6	2.233(2)	Cd2–O5	2.355(4)
Cd1–O7	2.365(3)	Cd2–O6	2.2379(19)
Cd3–N1 ^{iv}	2.288(3)	Cd3–O1	2.290(2)
Cd3–N2	2.508(3)	Cd3–O2 ^v	2.225(2)
Cd3–N5 ⁱⁱⁱ	2.498(3)	Cd3–O6 ⁱⁱ	2.274(2)
N4–Cd1–O7	87.39(9)	O6–Cd2–O5 ⁱⁱ	87.50(10)
N4 ⁱ –Cd1–O7	92.61(9)	O6–Cd2–O5	92.50(10)
N4–Cd1–O7 ⁱ	92.61(9)	O6 ⁱⁱ –Cd2–O6	180.0
N4 ⁱ –Cd1–O7 ⁱ	87.39(9)	O5 ⁱⁱ –Cd2–O5	180.0
N4–Cd1–N4 ⁱ	180.0	N1 ^{iv} –Cd3–O1	86.25(8)
O6 ⁱ –Cd1–O6	180.0	N1 ^{iv} –Cd3–N2	92.98(8)
O6 ⁱ –Cd1–N4	85.44(8)	N1 ^{iv} –Cd3–N5 ⁱⁱⁱ	95.63(8)
O6–Cd1–N4	94.56(8)	N5 ⁱⁱⁱ –Cd3–N2	171.35(10)
O6 ⁱ –Cd1–N4 ⁱ	94.56(8)	O2 ^v –Cd3–O6 ⁱⁱ	89.89(9)
O6–Cd1–N4 ⁱ	85.44(8)	O2 ^v –Cd3–N1 ^{iv}	99.95(9)
O6 ⁱ –Cd1–O7	94.62(9)	O6 ⁱⁱ –Cd3–N1 ^{iv}	169.85(8)
O6–Cd1–O7	85.38(9)	O2 ^v –Cd3–O1	170.07(8)
O6 ⁱ –Cd1–O7 ⁱ	85.38(9)	O6 ⁱⁱ –Cd3–O1	83.67(8)
O6–Cd1–O7 ⁱ	94.62(9)	O2 ^v –Cd3–N5 ⁱⁱⁱ	92.24(9)
O7–Cd1–O7 ⁱ	180.0	O6 ⁱⁱ –Cd3–N5 ⁱⁱⁱ	86.38(8)
N(3)–Cd(2)–O(5)	90.62(11)	O1–Cd3–N5 ⁱⁱⁱ	94.88(9)
N(3)–Cd(2)–O(5) ⁱⁱ	89.38(11)	O2 ^v –Cd3–N2	87.02(9)
N(3)–Cd(2)–N(3) ⁱⁱ	180.0	O6 ⁱⁱ –Cd3–N2	85.01(8)
O(6)–Cd(2)–N(3)	94.47(8)	O1–Cd3–N2	84.91(9)
O(6)–Cd(2)–N(3) ⁱⁱ	85.53(8)		
Complex 2			
Cd1–N3	2.434(2)	Cd1–O1	2.2977(13)
Cd1–O3 ^{viii}	2.236(2)	Cd2–O4	2.2211(11)
Cd1–O5	2.239(2)	Cd2–N2 ⁱⁱⁱ	2.3265(15)
Cd1–O4	2.2640(18)	Cd2–O2	2.4542(13)
O3 ^{viii} –Cd1–O5	106.72(7)	O1–Cd1–N3	84.90(4)
O3 ^{viii} –Cd1–O4	88.69(7)	N2 ⁱⁱⁱ –Cd2–O2	81.98(6)
O5–Cd1–O4	164.60(7)	N2 ^{iv} –Cd2–O2	98.02(6)
O3 ^{viii} –Cd1–O1	94.93(4)	N2 ⁱⁱⁱ –Cd2–N2 ^{iv}	180.0
O5–Cd1–O1	89.83(4)	O2 ^{ix} –Cd2–O2	180.0
O4–Cd1–O1	88.81(4)	O4–Cd2–O4 ^{ix}	180.0
O1–Cd1–O1 ⁱ	169.79(7)	O4–Cd2–N2 ⁱⁱⁱ	93.83(6)
O3 ^{viii} –Cd1–N3	168.38(8)	O4–Cd2–N2 ^{iv}	86.17(6)
O5–Cd1–N3	84.90(8)	O4–Cd2–O2 ^{ix}	74.13(5)
O4–Cd1–N3	79.69(7)	O4–Cd2–O2	105.87(5)
Complex 3			
Cd1–N1	2.306(3)	Cd1–O2	2.286(3)
Cd1–O1	2.299(3)	N1–Cd1–O2	86.88(12)
N1–Cd1–O1	88.85(12)	O2 ⁱ –Cd1–O2	180.0
N1 ⁱ –Cd1–O2	93.12(12)	O2–Cd1–O1 ⁱ	90.49(13)
N1 ⁱ –Cd1–O1	91.15(12)	O2–Cd1–O1	89.51(13)
N1–Cd1–N1 ⁱ	180.0	O1 ⁱ –Cd1–O1	180.0

Symmetry codes for **1**: i = $-x + 1$, $-y + 1$, $-z + 1$; ii = $-x + 2$, $-y + 1$, $-z + 1$; iii = $x + 1$, y , z ; v = x , $-y + 1/2$, $z + 1/2$; iv = $-x + 2$, $-y$, $-z + 1$; for **2**: i = x , $-y + 1/2$, z ; iii = $-x + 1$, $-y + 1$, $-z + 1$; iv = x , y , $z - 1$; viii = $-x + 2$, $-y + 1$, $-z$; ix = $-x + 1$, $-y + 1$, $-z$; for **3**: I = $-x + 1$, $-y$, $-z + 2$.

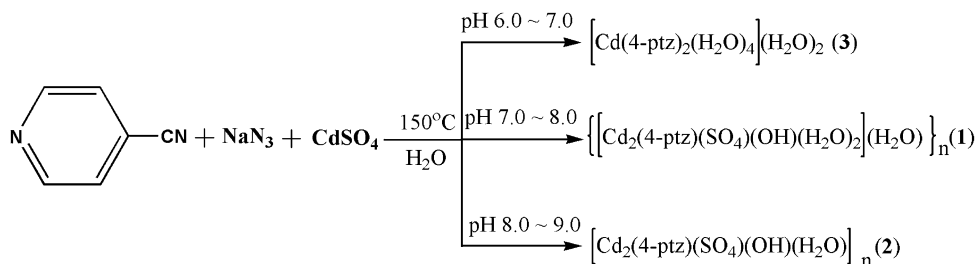
metal organic polymers **1** and **2**. Their phase purities of the bulk samples of these two compounds are confirmed by powder X-ray diffraction determination (figure S2), elemental analysis, and infrared absorption spectrum. Single-crystal X-ray diffraction analyses indicate that although **1** and **2** are both prepared using the same raw materials, their structures are

apparently different from each other. For comparison, a weak acid condition pH 6.0–7.0 is also carried out using diluted water solution of H₂SO₄ (0.01 M). X-ray diffraction result indicates that only a discrete mononuclear Cd(II) compound **3** is obtained, which has been reported earlier by Mautner *et al.* and Zou *et al.* [18, 25]. The completely different crystal structures of **1–3** reveal a significant influence of pH in their reaction medium on the supramolecular structure.

3.2. Description of crystal structure of **1**

For **1**, crystallized in monoclinic *P*2₁/*c* space group, its asymmetric unit is composed of three crystallographic unique Cd(II) cations, i.e. half-occupied Cd1/Cd2 and complete Cd3, one 4-ptz[−] anion ligand, one sulfate dianion, one μ₃-OH[−] group (O6), and two coordinated (O5 and O7) and one not coordinated (O8) water (figure 1). In the 4-ptz[−] moiety, tetrazole is twisted away from the pyridine ring with a dihedral angle 61.8(1)° between them. All three Cd(II) cations are six-coordinate, forming a distorted octahedral configuration. However, the donor set of coordination around Cd3 is distinct from that of Cd1 and Cd2 atoms. For both Cd1 and Cd2 located on inversion centers, they are coordinated by two nitrogens [Cd1–N4 2.328(3) Å, Cd2–N3 2.317(3) Å] from two symmetric 4-ptz[−] ligands, two end-on waters [Cd1–O7 2.365(3) Å, Cd2–O5 2.355(4) Å], and two μ₃-OH[−] groups [Cd1–O6 2.233(2) Å, Cd2–O6 2.2379(19) Å]. As for Cd3 cation, it is ligated by three nitrogens [Cd3–N2 2.508(3) Å, Cd3–N1^{iv} 2.288(3) Å, and Cd3–N5ⁱⁱⁱ 2.498(3) Å] from three separate 4-ptz[−] ligands and three oxygens from two sulfates [Cd3–O1 2.290(2) Å, Cd3–O2^v 2.225(2) Å] and one μ₃-OH[−] [Cd3–O6ⁱⁱ 2.274(2) Å] anion.

The Cd–N_{pyridine} [2.288(3) Å] is the shortest Cd–N bond and the 1- and 4-positioned tetrazole Cd–N bonds [2.498(3) and 2.508(3) Å] are the longest. The 2- and 3-positioned tetrazole Cd–N bonds lie between them [2.317(2) and 2.328(2) Å]. For Cd–O bonds, the average Cd–O_{water} bond [2.360(3) Å] is longer by *ca.* 0.11 Å than the mean value of Cd–O_{hydroxyl} bonds [2.248(2) Å]. When only the three Cd–O_{hydroxyl} bonds are considered, the Cd3–O bond is longer by 0.035 Å than the other two. Those cis angles around three Cd(II) centers vary from 85.38(9)° to 94.62(9)° for Cd1, 85.53(8)° to 94.47(8)° for Cd2, and 83.67(8)° to 99.95(9)° for Cd3. But trans angles are of ideal values of 180° for Cd1 and Cd2 atoms and 169.85(8)° to 171.35(10)° for Cd3, indicating Cd3 octahedron is slightly more distorted than that of the other two Cd(II) ions, attributed to the steric hindrance from these nitrogens from different positions of 4-ptz[−] when they are coordinated.



Scheme 1. The *in situ* synthesis of tetrazole ligand 4-ptz in **1–3**.

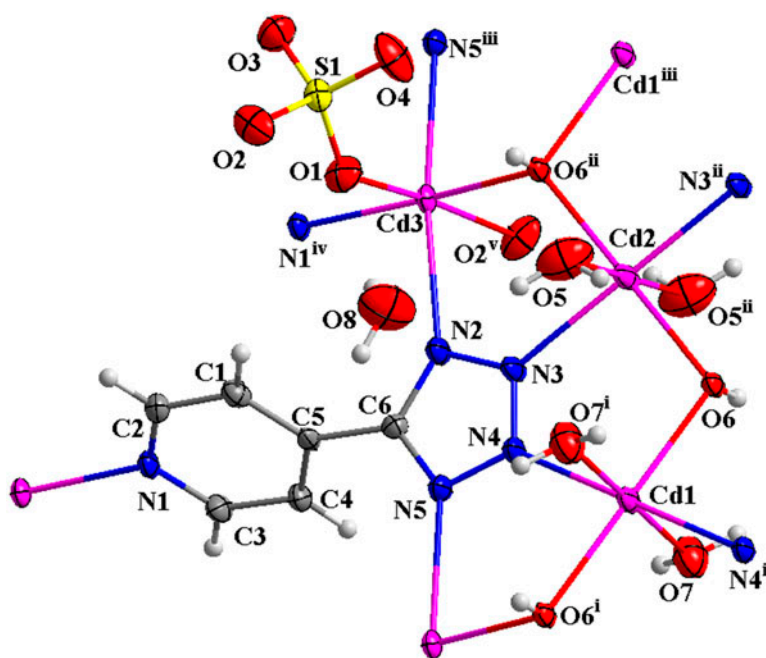


Figure 1. Coordination environment of three Cd(II) ions in **1** with all the non-hydrogen atoms shown as 50% thermal ellipsoid probabilities (symmetry codes: i = $1-x$, $1-y$, $1-z$; ii = $2-x$, $1-y$, $1-z$; iii = $1+x$, y , z ; iv = $2-x$, $-y$, $1-z$; v = x , $1/2-x$, and $1/2+z$).

The 4-ptz⁻ in **1** is coordinated to five Cd(II) centers in a pentadentate mode $\mu_5-k_{N1}:k_{N2}:k_{N3}:k_{N4}:k_{N5}$, which is only observed in a few cases by a detailed CSD search [26–28]. By 4-ptz⁻ and μ_3 -OH⁻ coordinated to metal centers simultaneously, a 2-D layer structure parallel to the (0 0 1) plane was constructed (figure 2). Adjacent 2-D layers were further joined by SO₄²⁻ anions in a bidentate $\mu_2-k_{O1}:k_{O2}$ mode ligated to two glide-plane-related Cd3 ions, resulting in the final 3-D polymer structure in **1** (figure 2). In the 3-D structure, due to existence of coordinated and coordination-free waters and μ_3 -OH⁻, extensive hydrogen bonds are furnished to the 3-D network (figure S3 and table S1). *Platon* analysis indicates that two stronger $\pi \dots \pi$ stacking interactions exist between two pairs of inversion center-related pyridine rings with their centroid-to-centroid distance of 3.539(2) and 3.687(2) Å.

3.3. Description of crystal structure of **2**

Compared with **1**, **2** was also crystallized in the monoclinic crystal system but with a space group $P2_1/m$. The pyridine and tetrazole groups in 4-tpz⁻ are almost coplanar with the dihedral angle of 0.12°. The asymmetric unit of **2** consists of two halves of Cd(II) cations, each half a 4-ptz⁻, SO₄²⁻, and μ_3 -OH⁻, and half an end on coordinated water. Except for Cd2 cation being dually symmetry-related by both a twofold skew axis and an inversion center, all the other component ions in **2** are symmetry-related by mirror planes. In the coordination spheres, both Cd1 and Cd2 adopt octahedral configurations with different donor sets.

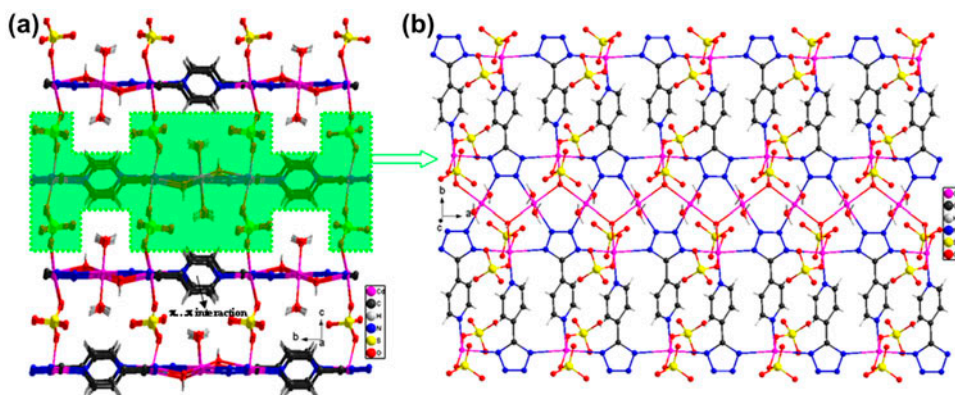


Figure 2. (a) Part of the crystal packing showing the formation of the 3-D polymer in **1** with $\pi \cdots \pi$ stacking interaction marked and (b) part of the crystal packing showing the formation of the 2-D layer structure parallel to the (0 0 1) plane by only μ_5 -4-ptz⁻ and μ_3 -OH⁻ bridging between Cd(II) centers.

For Cd1, the donor sets consist of one pyridine N3 of 4-ptz⁻, two mirror symmetry-related oxygens (O1) and another oxygen (O3) from three separate SO₄²⁻ anions, one μ_3 -bridging hydroxyl group (O4) and one end-on coordinated water (O5) (Figure 3). These five Cd–O bonds around Cd1 are 2.239(2)–2.298(2) Å, much shorter than the Cd1–N3 bond [2.434(2) Å]. The cis and trans angles in the octahedron around Cd1 are 79.7(2)°–106.71(2)° and 164.60(2)°–169.80(2)°, respectively. For Cd2, the six donors are from three pairs of inversion-related 2-positioned N2 of tetrazole groups, sulfate O2, and μ_3 -bridging hydroxyl O4. These Cd2–N2, Cd2–O2, and Cd–O4 bonds lengths are 2.327(2), 2.454(2), and 2.221(2) Å, respectively. The cis angles around Cd2 are 74.13(5)°–105.87(5)° and trans angles are all ideal 180°; the similar bond lengths and angle ranges around Cd1 and Cd2 indicate similar octahedral configurations around them. In comparison with the μ_5 -bridging mode of 4-ptz⁻ in **1**, the 4-ptz⁻ in **2** is coordinated to three metal centers (Cd1/Cd2/Cd2) in a μ_3 - k_{N2} : k_{N2} : k_{N3} mode. However, sulfate in **2** is coordinated to five neighboring Cd(II) ions in a μ_5 - k_{O1} : k_{O2}^2 : k_{O3} mode as rarely observed in analogs containing tetrazole groups [29–33]. The hydroxyl group in **2** was in a μ_3 -bridged mode similar to that in **1**, but the Cd...Cd distances linked by it in **2** [Cd1...Cd2 3.855(2) Å, Cd2...Cd2 3.475(2) Å] are slightly shorter than those in **1** [Cd1...Cd2 3.598(2) Å, Cd1...Cd3 3.892(2) Å, and Cd2...Cd3 3.909(2) Å], which may be mainly due to the steric requirement set by the condition environment.

In the crystal of **2**, the complex 3-D network can be analyzed in terms of three substructures. First, by a joint coordination of 2- and 3-positioned N2 of 4-ptz⁻ to Cd2 centers a 1-D chain-like structure along [0 1 0] was formed with a Cd2...Cd2 distance of 3.475(2) Å [figure 4(c)]. Second, metal Cd1 was similarly linked but by sulfate O1 and O3, forming the other chain along the [0 1 0] axis with the nearest Cd1...Cd1 distance of 5.326(2) Å [figure 4(b)]. As a result, these two kinds of chains were joined together by O2 of sulfate and μ_3 -OH⁻, giving a 2-D layer structure parallel to the (0 0 1) plane. Finally, these adjacent (0 0 1) layer structures were linked via coordination of pyridine N3 to Cd1, forming the 3-D polymer network in **2** [figure 4(a)]. In the network, each O–H...N hydrogen bond and C–H...O interaction are fewer than that in **1** because of only one water included in **2**.

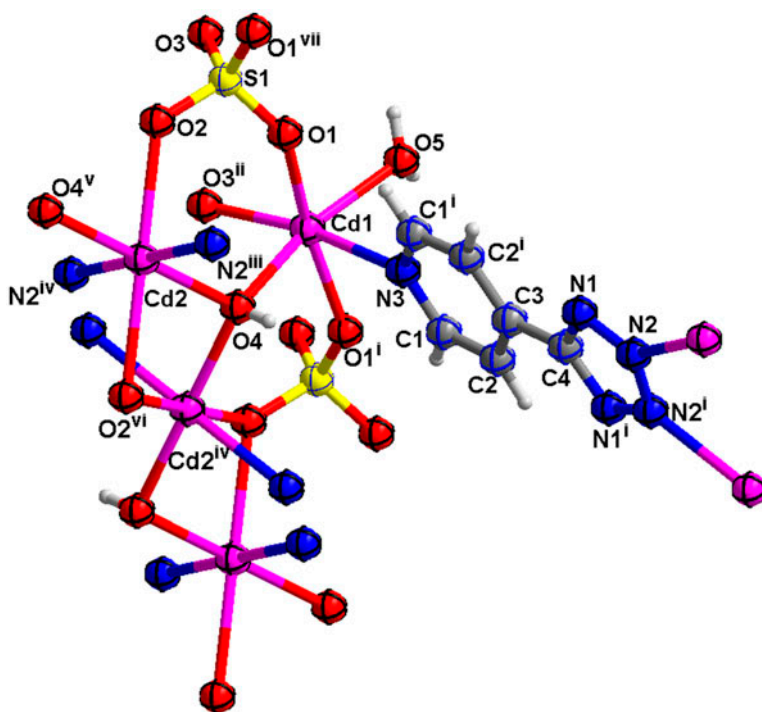


Figure 3. Coordination environment of Cd(II) ions in **2** with all non-hydrogen atoms shown as 50% thermal ellipsoid probabilities (symmetry codes: i = $x, 1/2 - y, z$; ii = $2 - x, y - 1/2, -z$; iii = $1 - x, 1 - y, 1 - z$; iv = $x, y, z - 1$; v = $1 - x, 1/2 + x, -z$; vi = $1 - x, y - 1/2, -z$; vii = $x, 3/2 - y, z$).

For **1** and **2**, both consist of a 3-D coordination network different from some tetrazole-cadmium-containing complexes, such as $[\text{Cd}(\text{pytz})_2(\text{H}_2\text{O})_4] \cdot 2\text{H}_2\text{O}$ [18], $[\text{Cd}(\text{pn})_2(\text{trans-AT})]$, and $[\text{Cd}(\text{en})_2(\text{trans-AT})] \cdot 4\text{H}_2\text{O}$ [34]. These three analogs are similarly assembled into the 2-D coordination networks in which their tetrazole moieties all adopt μ_2 -bridging mode. In comparison, in **1** and **2**, there are μ_4 - or μ_2 -bridging patterns for the tetrazole groups. The unique bridging modes and directionality of the ligand/ion such as 4-ptz^- in **1** and SO_4^{2-} in **2** may be the structural factor leading to the final 3-D assembly. The different coordination modes in **1** and **2** should be ascribed to the pH-directed reaction medium.

3.4. Topological analysis of **1** and **2**

In order to better understand the structure in **1**, the complex 3-D network can be topologically analyzed with Cd(II) centers regarded as six-connected nodes, and 4-ptz^- , OH^- , and SO_4^{2-} anions as five-, three-, and two-connected nodes, respectively. To obtain the final topologically simplified network, nodes less than or equal to two have been omitted. Thus, a deduced topological four-nodal (3,4,5,6)-connected network is given with a Schläfli symbol of $(4^3)(4^4.6^2)(4^4.6^6.8^5)(4^5.6^5)$ topology [figure 5(a)]. Similarly, the 3-D polymer network in **2** can be also analyzed topologically by considering Cd1 as a five-connected node, Cd2 as a six-connected node, 4-ptz^- and hydroxyl as three-connected nodes, and SO_4^{2-} anion as

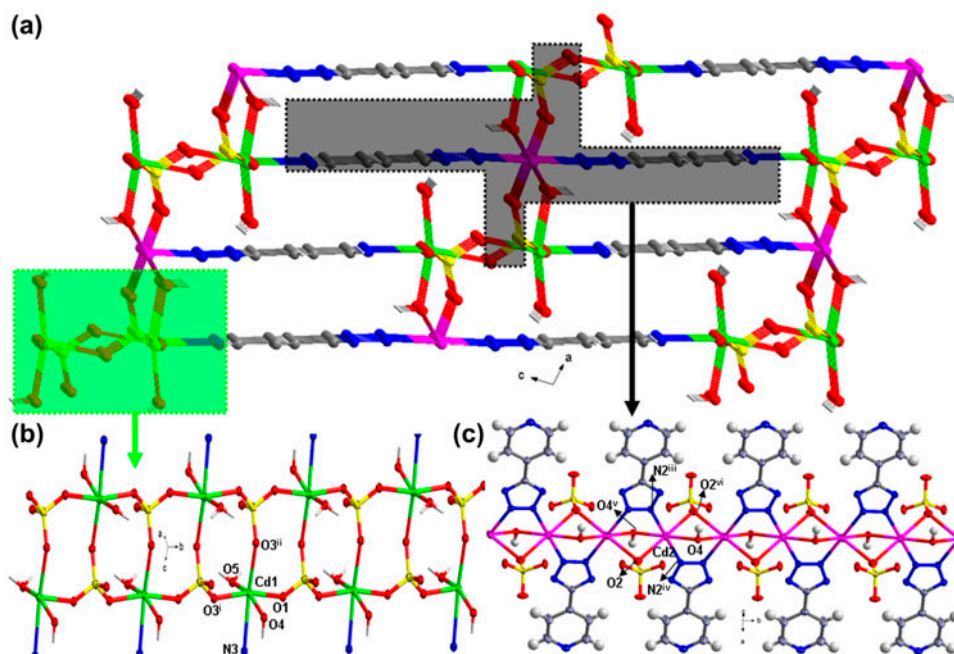


Figure 4. Part of the crystal packing showing the formation of the 3-D polymer structure in **2** (a); Part of the 1-D chain-like structure linked by only sulfate anions along the $[0\ 1\ 0]$ axis (b); another 1-D chain-like structure linked by sulfate, hydroxyl, and 4-ptz anions along the $[0\ 1\ 0]$ axis (c) (symmetry codes: i = $x, 1/2 - y, z$; ii = $2 - x, y - 1/2, -z$; iii = $1 - x, 1 - y, 1 - z$; iv = $x, y, z - 1$; v = $1 - x, 1/2 + x, -z$; vi = $1 - x, y - 1/2, -z$).

five-connected nodes. Thus, the final simplified network can be given as an unprecedented five-nodal $(3,3,5,5,6)$ -c T2 net with the short and long Schäfli symbol of $(4.8^2)(4^3)(4^4.6^2.8^4)(4^5.6^5)(4^8.6^6.8)$ and $(4.4.4_2)(4_2.8_{13}.8_{13})(4.4.4.4.4_2.8.8.8_3.8_3.8_3)(4.4.4.4.6_2.8_2.8_6.8_9.8_9.8_9.8_9)$, respectively [figure 5(b)]. To the best of our knowledge, these two types of topological networks for **1** and **2** are not reported previously.

3.5. pH Effect on the formation of 1–3

By analyzing crystal structures of **1** and **2**, several structural similarities are found, with all having octahedral configuration around Cd(II), the same components, *in situ* formation of 4-ptz, and spontaneous involvement of μ_3 -bridging OH^- and water molecules in their crystals. However, the differences between them are significant: (i) Synthesis strategy – by a systematic and careful study, it can be concluded that with increasing of pH, this one-pot hydrothermal reaction prefers formation of 3-D coordination polymers **1** and **2** relative to the mononuclear Cd(II) complex **3**. (ii) Water involvement – with the pH value increased from 6.0–7.0 to 8.0–9.0, from weak acidic to weak alkaline, the water content becomes less and less in a trend of $\mathbf{3} < \mathbf{1} < \mathbf{2}$. (iii) Coordination mode – the variations of reaction pH from acid to alkaline strongly influence the coordination modes of 4-ptz and SO_4^{2-} (vide ante). The main reason may come from the much easier deprotonation of 4-ptz ligand in an alkaline solution of **1** and **2** than that in **3**. With an attempt to ascertain the strong acidic (pH < 6.0) and alkaline (pH > 9.0) effects on the supramolecular assembly, we failed

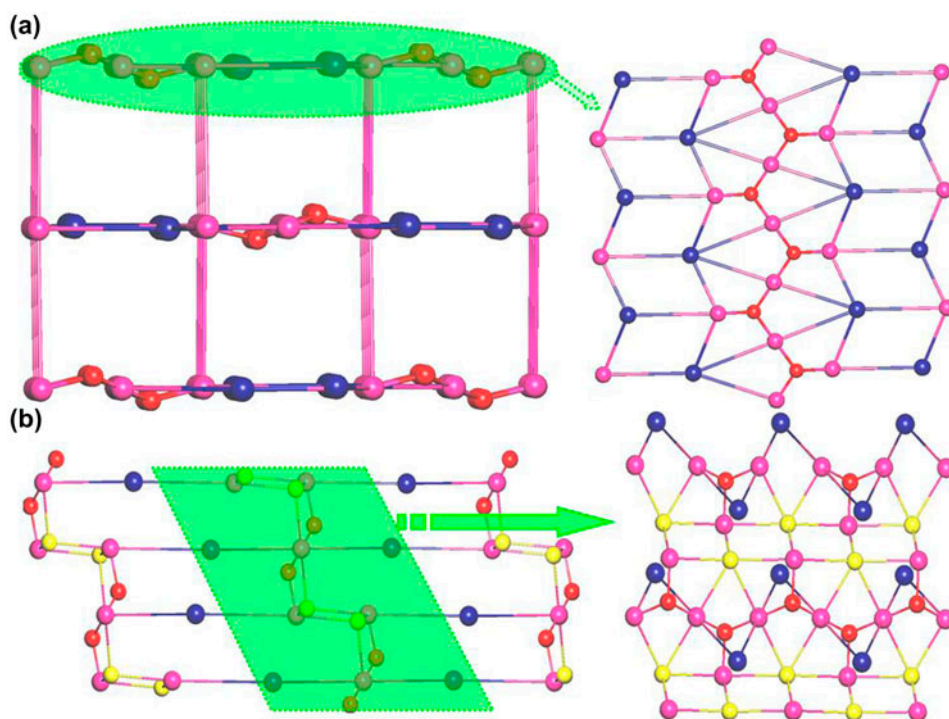


Figure 5. (a) Topological simplification of the 3-D coordination network in **1** with only more than two-connected nodes being shown. These pink, blue, and red balls represent the metal Cd atoms, 4-ptz⁻ ligand, and μ_3 -OH⁻ group, respectively and (b) topological simplification of the 3-D coordination network in **2** with only more than three-connected nodes being shown. These pink, blue, yellow, and red balls represent the Cd ions, 4-ptz⁻ ligand, SO₄²⁻ anion, and μ_3 -OH⁻ group, respectively (see <http://dx.doi.org/10.1080/00958972.2015.1024668> for color version).

several times. For the former, the residual solution becomes clear when the reaction is finished. For the latter, only some microcrystallized powder samples are obtained. The pH in this *in situ* reaction is a determinant factor for the formation of **1–3** with pH changing from 6.0 to 9.0.

3.6. Thermogravimetric analysis of **1** and **2**

The TGA measurements show that **1** begins to decompose at 120 °C and displays two main stages of mass loss (figure S4). The first weight loss of 9.27% (Calcd 10.0%) from 120 to 250 °C is consistent with the release of the two coordination-free and coordinated waters. The second can be attributed to degradation of 4-ptz above 300 °C. Due to decomposition of the polymer, the total observed weight loss to 830 °C is 51.7%, indicating that the final decomposed residual should be inorganic metal oxide CdO. For **2**, the thermal decomposition is similar to that of **1** except for water release between 160 and 330 °C. The following several processes from 330 to 840 °C should be due to decomposition of 4-ptz⁻, SO₄²⁻, and OH⁻, even though it seems to be more complicated than in **1**. The final percent composition of 49.5% indicates the residual is also CdO. The analysis we have made leads to the

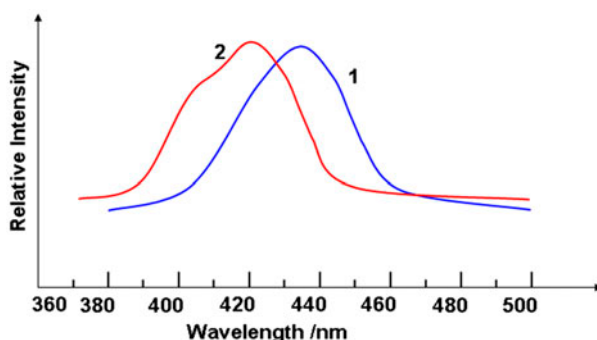


Figure 6. Fluorescent emission spectra of **1** (blue) and **2** (red) (see <http://dx.doi.org/10.1080/00958972.2015.1024668> for color version).

conclusion that both compounds are stable in air and may be suitable for further investigation as functional materials.

3.7. Luminescent properties of **1** and **2**

Metal organic compounds containing d^{10} electron for metal ions exhibit excellent luminescent properties. Thus, the photoluminescent characteristics of **1** and **2** in the solid state were evaluated. When **1** and **2** are excited at 372 and 366 nm, respectively, they show maximum emission at wavelengths 435 and 420 nm (figure 6). In comparison with the free 4-ptz ligand (excited: 350 nm; emission: 519 nm) [35], the maximum emission peaks of both compounds have significant blue shifts by 84 nm for **1** and 99 nm for **2**. An earlier similar emission was assigned to intraligand electron transition for the analog, $[\text{Zn}(\text{OH})(4\text{-ptz})]_n$ [36]. However, following some reported Cd(II) analogs and from our careful determinations [37–39], these two similar intense and broad bands in **1** and **2** may be mainly attributed to ligand-to-ligand electronic transition. The probable reasons are when 4-ptz⁻ coordinates to Cd(II), it could increase the energy level between the highest occupied molecular orbital and the lowest unoccupied molecular orbital via increasing ligand rigidity. Indeed, adjacent ligand-to-ligand interaction has been observed through $\pi\cdots\pi$ stacking in our cases. The fluorescent variations of maximum emission for **1** and **2** can be tentatively assigned resulting from intrinsic linking modes, such as Cd-tetrazole-OH moieties, OH⁻, and SO₄²⁻ ions. Water molecules also affect the luminescence [40]. The photoluminescent emissions of **1** and **2** in the blue region can make them potential candidates for photoactive materials.

4. Conclusion

Two 3-D coordination polymers have been hydrothermally synthesized via *in situ* reactions under different pH conditions by employing CdSO₄, 4-cyanopyridine, and sodium azide as initial reactants. The combined results indicate that the pH strongly affects the assembly of

the final supramolecular structure. In a weak acid medium, only the mononuclear Cd(II) compound **3** is produced. However, 3-D compounds **1** and **2** can be prepared in alkaline conditions. The thermal stabilities and fluorescent properties show that both **1** and **2** may be used as potential optical materials in the blue light region. Further research will concentrate on the relationships between structures and their properties.

Supplementary material

Hydrogen-bonding parameters of **1–3** (table S1), crystal shapes of **1** and **2** (figure S1), experimental and simulated PXRD patterns for **1** and **2** (figure S2), crystal packing of **1** (figure S3), and TG curves of **1** and **2** (figure S4) are available as electronic supplementary information in the online version. CCDC-1025268 (**1**), 1025268 (**2**) and 1025268 (**3**) contain the supplementary crystallographic data for this article. These data can be obtained free of charge from the Cambridge Crystallographic Data Center via www.ccdc.cam.ac.uk/data_request/cif or E-mail: deposit@ccdc.cam.ac.uk.

Acknowledgement

Thanks to Dr Meng Xiang-Gao for his helpful discussions about crystal structures of all the compounds.

Disclosure statement

No potential conflict of interest was reported by the authors.

Funding

This work was supported by the National Natural Science Foundation of China [grant number 51172085]; “863” National Project of China [grant number 2013AA031903].

References

- [1] H. Zhao, Z.-R. Qu, H.-Y. Ye, R.-G. Xiong. *Chem. Soc. Rev.*, **37**, 84 (2008).
- [2] X.-M. Chen, M.-L. Tong. *Acc. Chem. Res.*, **40**, 162 (2006).
- [3] W. Zhang, R.-G. Xiong. *Chem. Rev.*, **112**, 1163 (2011).
- [4] F.A. Almeida Paz, J. Klinowski, S.M.F. Vilela, J.P.C. Tomé, J.A.S. Cavaleiro, J. Rocha. *Chem. Soc. Rev.*, **41**, 1088 (2012).
- [5] R.-G. Xiong, X. Xue, H. Zhao, X.-Z. You, B.F. Abrahams, Z. Xue. *Angew. Chem. Int. Ed.*, **114**, 3954 (2002).
- [6] W. Ouellette, J. Zubietta. *Chem. Commun.*, **30**, 4533 (2009).
- [7] W.-C. Song, Q. Pan, P.-C. Song, Q. Zhao, Y.-F. Zeng, T.-L. Hu, X.-H. Bu. *Chem. Commun.*, **46**, 4890 (2010).
- [8] M. Dincă, A. Dailly, J.R. Long. *Chem. Eur. J.*, **14**, 10280 (2008).
- [9] B. Zheng, H. Dong, J. Bai, Y. Li, S. Li, M. Scheer. *J. Am. Chem. Soc.*, **130**, 7778 (2008).
- [10] W. Ouellette, H. Liu, C.J. O'Connor, J. Zubietta. *Inorg. Chem.*, **48**, 4655 (2009).
- [11] W. Zhang, F. Zhao, T. Liu, M. Yuan, Z.-M. Wang, S. Gao. *Inorg. Chem.*, **46**, 2541 (2007).
- [12] X.-S. Wang, Y.-Z. Tang, X.-F. Huang, Z.-R. Qu, C.-M. Che, P.W.H. Chan, R.-G. Xiong. *Inorg. Chem.*, **44**, 5278 (2005).
- [13] S.-T. Wu, L.-S. Long, R.-B. Huang, L.-S. Zheng. *Cryst. Growth Des.*, **7**, 1746 (2007).

- [14] N. Matsumoto, Y. Motoda, T. Matsuo, T. Nakashima, N. Re, F. Dahan, J.-P. Tuchagues. *Inorg. Chem.*, **38**, 1165 (1999).
- [15] J. Sha, J. Peng, Y. Lan, Z. Su, H. Pang, A. Tian, P. Zhang, M. Zhu. *Inorg. Chem.*, **47**, 5145 (2008).
- [16] Q.-Y. Li, M.-H. He, Z.-D. Shen, G.-W. Yang, Z.-Y. Yuan. *Inorg. Chem. Commun.*, **20**, 214 (2012).
- [17] L. Zhang, Z.-J. Li, Y.-Y. Qin, J. Zhang, J.-K. Cheng, P.-X. Yin, Y.-G. Yao. *J. Mol. Struct.*, **891**, 138 (2008).
- [18] J.H. Zou, H. Wu, D.L. Zhu, H. Tian, P. Zhang, L.Y. Zhao, Z.W. Ruan, J. Xie, Q.Y. Li, G.W. Yang. *J. Coord. Chem.*, **67**, 3444 (2014).
- [19] M. Li, Z. Li, D. Li. *Chem. Commun.*, **29**, 3390 (2008).
- [20] F. Himo, Z.P. Demko, L. Noodleman, K.B. Sharpless. *J. Am. Chem. Soc.*, **124**, 12210 (2002).
- [21] F. Himo, Z.P. Demko, L. Noodleman, K.B. Sharpless. *J. Am. Chem. Soc.*, **125**, 9983 (2003).
- [22] Bruker. *SMART and SAINT PLUS*. Bruker AXS Inc, Madison, WI (2002).
- [23] G.M. Sheldrick. *Acta Cryst. A*, **64**, 112 (2008).
- [24] A.L. Spek. *J. Appl. Crystallogr.*, **36**, 7 (2003).
- [25] F.A. Mautner, C. Gspan, K. Gatterer, M.A.S. Goher, M.A.M. Abu-Youssef, E. Bucher, W. Sitte. *Polyhedron*, **23**, 1217 (2004).
- [26] X. Wang, J. Peng, M.-G. Liu, D.-D. Wang, C.-L. Meng, Y. Li, Z.-Y. Shi. *CrystEngComm*, **14**, 3220 (2012).
- [27] G.-X. Meng, J.-H. Zhu, Y.-M. Feng, X.-T. Huang, H.-L. Yang. *Acta Cryst. C*, **68**, m194 (2012).
- [28] Z.-Y. Liu, X.-J. Shi, E.-C. Yang, X.-J. Zhao. *Inorg. Chem. Commun.*, **13**, 1259 (2010).
- [29] W. Ouellette, B.S. Hudson, J. Zubieta. *Inorg. Chem.*, **46**, 4887 (2007).
- [30] W. Ouellette, A.V. Prosvirin, J. Valeich, K.R. Dunbar, J. Zubieta. *Inorg. Chem.*, **46**, 9067 (2007).
- [31] Z. Li, M. Li, X.-P. Zhou, T. Wu, D. Li, S.W. Ng. *Cryst. Growth Des.*, **7**, 1992 (2007).
- [32] G. Hong-You, L. Zeng-He, L. Xiu-Yan, Z. Chang-Yuan, W. Ru-Ji. *Chin. J. Chem.*, **21**, 466 (2003).
- [33] Y.-L. Yao, L. Xue, Y.-X. Che, J.-M. Zheng. *Cryst. Growth Des.*, **9**, 606 (2008).
- [34] W.B. Chen, H. Wu, Y.X. Qiu, X.M. Lin, M. Yang, H. Yan, F.X. Gao, Z.J. Ou Yang, W. Dong. *J. Coord. Chem.*, **66**, 1700 (2013).
- [35] X.-L. Wang, N. Li, A.-X. Tian, J. Ying, T.-J. Li, X.-L. Lin, J. Luan, Y. Yang. *Inorg. Chem.*, **53**, 7118 (2014).
- [36] J.M. Seco, M. de Araújo Farias, N.M. Bachs, A.B. Caballero, A. Salinas-Castillo, A. Rodríguez-Diéguez. *Inorg. Chim. Acta*, **363**, 3194 (2010).
- [37] J.-Q. Sha, J.-W. Sun, C. Wang, G.-M. Li, P.-F. Yan, M.-T. Li, M.-Y. Liu. *CrystEngComm*, **14**, 5053 (2012).
- [38] Y. Lu, Y. Xu, E. Wang, J. Lü, C. Hu, L. Xu. *Cryst. Growth Des.*, **5**, 257 (2004).
- [39] H. Jin, Y. Qi, E. Wang, Y. Li, X. Wang, C. Qin, S. Chang. *Cryst. Growth Des.*, **6**, 2693 (2006).
- [40] R.-B. Zhang, Z.-J. Li, Y.-Y. Qin, J.-K. Cheng, J. Zhang, Y.-G. Yao. *Inorg. Chem.*, **47**, 4861 (2008).